Ocean Dynamics (2014) 64:293–300
DOI 10.1007/s10236-013-0686-1

Numerical study on wave propagation over a fluid-mud layer with different bottom conditions

Xiaojing Niu · Xiping Yu

Received: 28 February 2012 / Accepted: 23 December 2013 / Published online: 12 January 2014

Abstract Wave decay over a muddy seabed has been widely reported. In previous studies, the fluid-mud layer is usually treated as a homogeneous layer with a certain thickness lying on the rigid bottom. However, the muddy seabed beneath a fluid-mud layer is usually movable in practice. This study aims to find out the influence of the movable seabed beneath a fluid-mud layer. For this purpose, a numerical model for wave propagation over a multilayered muddy seabed is developed, in which water is treated as a Newtonian fluid, and the rheology of mud is described by a visco-elastic–plastic model. The laboratory experiments of Sakakiyama and Bijker (J Waterw Port Coast Ocean Eng 115(5):614–633, 1989) are chosen to validate the numerical model. The model is then employed to investigate the movement of a fluid-mud layer with different conditions of the underlying mud layer and its influence on wave decay. It is found that the underlying mud layer plays a very important role in the wave–mud interaction and greatly affects the wave decay rate.

Keyword Wave–mud interaction · Wave decay · Multilayered muddy seabed · Numerical model

1 Introduction

Muddy coasts are widely distributed in the world. At a muddy coast, fine sediments can be easily entrained into water during storms. The newly settled fine sediments on the seabed usually form high concentration slurry, i.e., the fluid-mud, in which further settlement of fine sediments is substantially hindered. Fluid-mud can be easily transported by gravity and by wave motion and deposits in deep areas such as navigation channels. After a storm, fluid-mud can exist for quite a long time and be dewatered gradually. Mehta et al. (1994) provided a schematic diagram showing the vertical variation of the mud density in the coastal environment, in which the muddy seabed was divided into three layers, i.e., a fluid-mud layer, a denser deforming bed, and a stationary bed. The seabed beneath the newly formed fluid-mud layer could have been formed for days or even months, so it can be in different conditions and behave differently as a consolidated muddy bed, a mud layer with larger density, or a mud layer with slightly larger density.

As waves pass over a muddy seabed, the oscillatory motion of the movable mud layers usually causes significant dissipation of wave energy. This important phenomenon has been studied by a number of researchers over the past decades. Usually, the muddy seabed is simplified as a homogeneous movable mud layer lying on a stationary horizontal bottom. Gade (1958) developed a two-layer model and studied the attenuation of linear water waves. In Gade's model, the upper layer, or the water, is treated as an inviscid fluid and the lower layer, or the mud, is assumed to be a viscous fluid. The analytical studies of the two-layer fluid model have been improved to make the model more realistic in the last decades, and a number of progresses have been achieved. Dalrymple and Liu (1978) improved the two-layer model by considering the viscosity of water. Owing to the complexity of the rheological property of the real mud, a number of advanced rheology models have been introduced to describe the behavior of the lower mud layer, including the visco-elastic model (Macpherson 1980; Maa and Mehta 1988), the Bingham fluid model (Mei and Liu 1987; Zhao and Lian 1994), the power-law pseudo plastic model (Huang et al. 2006), and the visco-

Responsible Editor: Qing He

This article is part of the Topical Collection on the *11th International Conference on Cohesive Sediment Transport*

X. Niu (✉) · X. Yu
Department of Hydraulic Engineering, Tsinghua University, Beijing, China
e-mail: nxj@tsinghua.edu.cn

X. Yu
e-mail: yuxiping@tsinghua.edu.cn

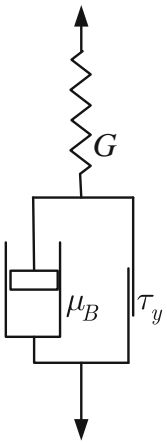

Fig. 1 Schematic description of the visco-elastic–plastic model

elastic–plastic model (Shibayama et al. 1990). There are also studies considering different wave conditions. For instance, the attenuation of solitary waves was studied by Jiang and Zhao (1989), and that of cnoidal waves was studied by Jiang et al. (1990). All these studies are analytical and are limited to the horizontal bed and the regular wave theories. Therefore, it may be of great importance to develop a numerical method for the interaction between waves and muddy bed, which can be used to simulate complicated seabed topography and various wave conditions.

Recently, analytical solutions of wave energy dissipation based on existing wave mud interaction models have also been used to extend the phase averaged wave models to deal with muddy coasts (Hall and Oveisy 2007; Winterwerp et al. 2007; Niu and Yu 2008a; Rogers and Holland 2009). This kind of models is useful in practice. However, it is necessary to point out that the wave energy dissipation is largely affected by the thickness of the fluid-mud layer. A small difference in mud thickness may lead to a significant difference in wave height distribution (Niu and Yu 2008a). Besides the thickness of the upper fluid-mud layer, the property of the muddy bed beneath the fluid-mud layer cannot be ignored either.

In this study, a numerical model for wave propagation over a muddy seabed is developed to study the influence of the underlying mud layer on the wave induced movement of the fluid-mud layer and the water surface wave decay. In the following sections, the numerical model is first described. Then, the model is validated by the laboratory experiments of Sakakiyama and Bijker (1989). Finally, three hypothetical muddy seabed cases considering a fluid-mud layer with different bottom conditions are studied, and the influence of the underlying muddy seabed on the wave decay rate are discussed based on the numerical results.

2 Mathematical model

2.1 Governing equations

The movement of water and mud are governed by the continuity equation and the equations of motion for incompressible continuum.

$$\frac{\partial u_j}{\partial x_j} = 0 \tag{1}$$

$$\rho\frac{\partial u_j}{\partial t} + \rho u_i\frac{\partial u_j}{\partial x_i} = \rho f_j - \frac{\partial p}{\partial x_j} + \frac{\partial \tau_{ij}}{\partial x_i} \tag{2}$$

where the indices i,j=1,2, follow the summation convention; x_i are the Cartesian coordinates, and t is time; u_i are the velocity components, and f_i are the body forces; ρ is the density; p is the pressure; τ_{ji} are the deviatoric stresses. The Newtonian fluid model is adopted for water.

$$\tau_{ij} = 2\mu_0 e_{ij} \tag{3}$$

where μ_0 is the viscosity;

$$e_{ij} = \frac{1}{2}\left(\frac{\partial u_i}{\partial x_j} + \frac{\partial u_j}{\partial x_i}\right) \tag{4}$$

is the rate-of-strain tensor.

The rheology of mud is complex and varies with its density and many other factors. In this study, the visco-elastic–plastic model introduced by Niu and Yu (2008b) is used to describe the rheological behavior of the mud. The visco-elastic–plastic model, as shown in Fig. 1, represents a material that is essentially elastic before yield and becomes visco-elastic after yield.

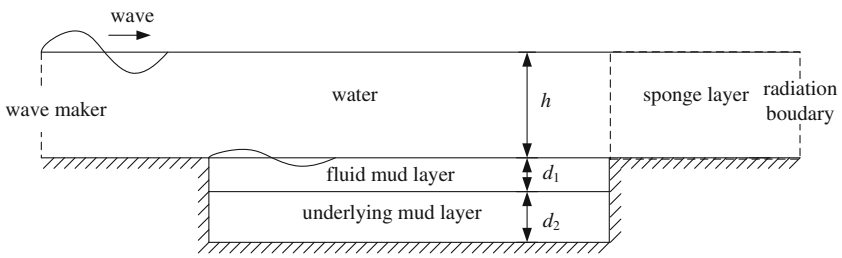

Fig. 2 Sketch of the computational domain

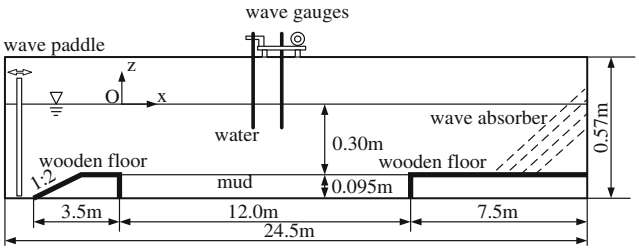

Fig. 3 Experimental setup of Sakakiyama and Bijker (1989)

The relevant constitutive equation can be written as

$$\begin{cases} \left(1-\dfrac{\tau_y}{\sqrt{J_2}}\right)\dfrac{\tau_{ij}}{2\mu_B}+\dfrac{1}{2G}\dfrac{d\tau_{ij}}{dt}=e_{ij}, & \left(\sqrt{J_2}>\tau_y\right) \\ \dfrac{1}{2G}\dfrac{d\tau_{ij}}{dt}=e_{ij}, & \left(\sqrt{J_2}\le\tau_y\right) \end{cases} \tag{5}$$

where μ_B is the viscosity in the visco-elastic–plastic model, τ_y is the yield stress of the mud, G is the elastic modulus of the mud, and J_2 is the second invariant of the deviatoric stress tensor. This rheological model can be reduced to a viscous model as $G\to\infty$ and $\tau_y=0$.

2.2 Surface and interface tracking

The problem of interest in the present study is shown in Fig. 2. All the subdomains, i.e., the water layer, the fluid-mud layer, and the underlying mud layer, are governed by Eqs. (1) and (2). In the subdomain occupied by water, the stresses are determined by Eq. (3), while in the subdomains occupied by mud, the stresses are determined by Eq. (5). Since the stresses and velocity components are all continuous in the entire domain, there is no need to exert a dynamic boundary condition at the interface between the water and the mud, beyond a unified treatment of Eqs. (1) and (2).

In this study, the free water surface is described by the VOF function. In the present case, the VOF function $F(x,z,t)$ is defined so that $F=1$ implies a position occupied by fluid, and $F=0$ implies a position occupied by air. The VOF function satisfies

$$\frac{\partial F}{\partial t}+\frac{\partial(uF)}{\partial x}+\frac{\partial(wF)}{\partial z}=0 \tag{6}$$

where x and z are the horizontal and the vertical coordinates; u and w are the horizontal and vertical velocity components. Equation (6) is solved with the donor–acceptor method (Hirt and Nichols 1981).

The water–mud interface and the interfaces between different mud layers are indicated by the volumetric sediment concentration. The volumetric sediment concentration S_v is also governed by the convection equation.

$$\frac{\partial S_v}{\partial t}+\frac{\partial(uS_v)}{\partial x}+\frac{\partial(wS_v)}{\partial z}=0. \tag{7}$$

In order to handle both the mild variation of sediment concentration inside a mud layer and the sharp variation at the interface between mud layers, a unique numerical method for the convection equation of sediment concentration is developed, which combines the Essentially Non-oscillatory Scheme (ENO) and Youngs' reconstruction scheme. Detailed information can be found in Niu (2008).

2.3 Boundary conditions and numerical methods

The computational domain is shown in Fig. 2. At the incident wave boundary, the instantaneous water depth and velocity are given based on the fifth-order Stokes wave theory. The right boundary is assumed to be non-reflective, and the Sommerfeld radiation condition is specified. Since the wave is not necessarily regular at the boundary due to the complicated response of the seabed, and also because of the difficulties in wave celerity estimation, a subregion with artificial dissipation is added in front of the right boundary to enhance the non-reflective boundary condition. The slip condition is applied to the fixed bed contacted with water, and the no-slip condition is applied to the fixed bed contacted with mud.

The main computational efforts of the numerical model are to solve the velocity and pressure. The numerical method is the same as that adopted in the study of Niu and Yu (2010). It is based on the well-known SMAC method, but the discretization of the momentum equations is replaced by a weighted implicit scheme to achieve a better stability, which is definitely necessary when mud with very large viscosity is involved. Spatial discretization is carried out over a staggered

Table 1 Selected cases of Sakakiyama and Bijker's (1989) experiments

Case	Density of mud ρ_m (kg/m^3)	Water depth h (m)	Thickness of mud layer d (m)	Wave period T (s)	Incident wave height H_0 (m)	Kinematic viscosity of mud ν (m^2/s)
A7	1,370	0.30	0.09	0.7~2.0	0.010~0.040	0.015
B2	1,300	0.30	0.09	0.6~2.0	0.010~0.037	0.010
C4	1,240	0.30	0.09	0.6~2.0	0.010~0.034	0.004
D4	1,150	0.30	0.09	0.6~2.0	0.010~0.034	0.001

Table 2 Parameters in the viscous fluid model

Case	Wave		Mud	
	Incident wave height H_0 (m)	Wave period T (s)	Density ρ_m (kg/m^3)	Kinematic viscosity ν (m^2/s)
A7	0.04 0.01	1.0	1,370	0.015
B2	0.035 0.020 0.010		1,300	0.010
C4	0.03 0.019 0.01		1,240	0.004
D4	0.032 0.020 0.010		1,150	0.001

mesh. The advection–diffusion equations are solved with a hybrid method combining the upwind scheme and the second-order central scheme. The Poisson equation is discretized with the classical five-point difference scheme.

3 Model validation

The laboratory experiments carried out by Sakakiyama and Bijker (1989) in a wave flume, as shown in Fig. 3, are used for the verification of the present model. Available cases of Sakakiyama and Bijker's experiments with a variety of properties of mud and wave conditions are summarized in Table 1. The cases were originally named as CASE A7, CASE B2, CASE C4, and CASE D4 by Sakakiyama and Bijker (1989) according to the physical properties of the mud and the items measured. All the original notations are retained here in order to avoid confusion. It may be worthwhile to mention that the

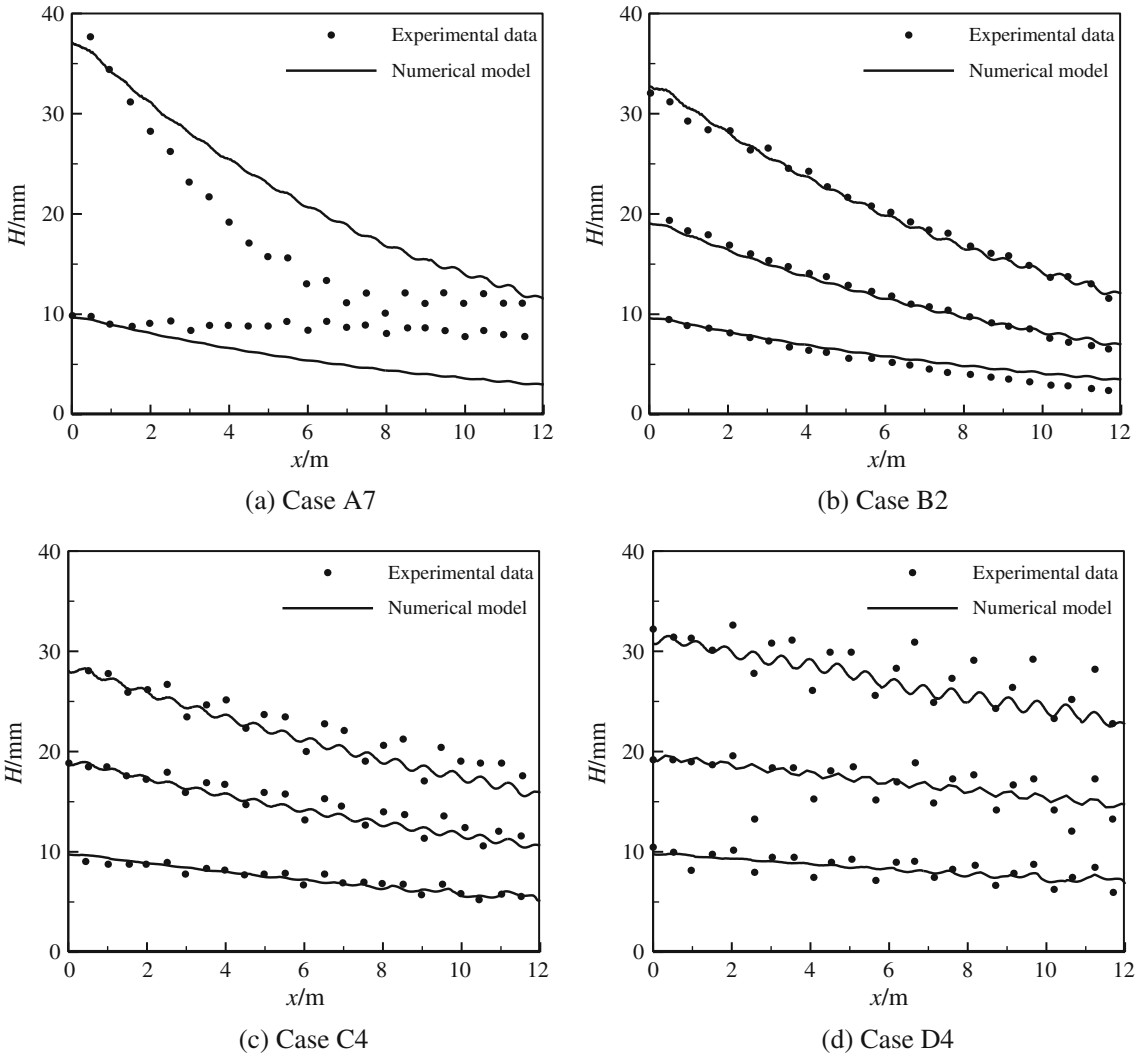

Fig. 4 Computed wave height along x axis by the Newtonian mud model

Table 3 Parameters in the visco-elastic–plastic model

Case	Wave		Mud			
	Incident wave height (m)	Wave period (s)	Density (kg/m^3)	Yield stress τ_y (pa)	Bingham viscosity μ_B (Pa·s)	Elastic modulus G (pa)
A7	0.04 0.01	1.0	1,370	12	8	500
C4	0.03 0.02 0.01		1,240	1	4	30

values of the apparent kinematic viscosity listed in Table 1 were measured under a shear rate of 1 s^{-1}.

First, mud is treated as a viscous fluid. The computational conditions are shown in Table 2. The measured apparent viscosity of mud, $\mu_0=\rho_m\nu$, is used in the numerical model. Figure 4 shows the numerical results of wave attenuation using the viscous fluid model to describe the mud, in comparison with Sakakiyama and Bijker's (1989) experimental data. The numerical results are in fairly good agreement with the experimental data when the mud is of low density (ρ_m= 1,300 kg/m^3, 1,240 kg/m^3, 1,150 kg/m^3) or small viscosity (ν=0.010 m^2/s, 0.004 m^2/s, 0.001 m^2/s). However, the difference between the numerical results and the experimental data becomes intolerable when the density and viscosity of the mud take relatively large values (CASE A7, ρ_m=1,370 kg/m^3, ν=0.015 m^2/s), no matter whether the wave height is large or small. In CASE A7, no significant attenuation is observed in the experiment when the wave height is small, i.e., the observed wave decay rate is much smaller than that predicted by the viscous fluid model. However, when the wave height is large, the observed wave attenuation is much more rapid than that predicted by the viscous fluid model.

To improve the performance of the numerical model, it is worthwhile to note that the mud barely moves in the experiment when the surface wave height is smaller than about 0.01 m in CASE A7. It is then reasonable to speculate that there is a significant change in mud properties under different wave height, especially for mud with relatively large density. The viscous fluid model is not applicable to this type of mud, and a visco-elastic–plastic model becomes necessary. In this study, the visco-elastic–plastic model shown in Fig. 1 is adopted. Table 3 shows the parameters in the visco-elastic–plastic model used in the computations. The parameters cannot be directly obtained from Sakakiyama and Bijker (1989). An (1993) compared the Bingham viscosity and the yield stress of the mud with the same density obtained by different investigators and found that a very big difference could reasonably exist. An (1993) pointed out that scattering of the experimental data may be caused by the difference in mineral components of the mud and also by the measuring method. The yield stress may also be very sensitive to the variation in water content of the mud. So the parameters in the visco-elastic–plastic model are guessed based on the existing experimental data. The visco-elastic–plastic model used in the present study represents that the mud is essentially elastic before yield and visco-elastic after yield. So the mud would behave as an elastic material without energy loss when the local wave height is small or the yield stress of the mud is large. In general, denser mud should have larger yield stress and elastic modulus. The apparent kinematic viscosity under a shear rate of 1 s^{-1} calculated using guessed parameters for each kind of mud should be consistent with the values provided by Sakakiyama and Bijker (1989). For CASE A7, the parameters are τ_y=12 Pa, μ_B=8 Pa·s, and G=500 Pa. For Case C4, the parameters are τ_y=1 Pa, μ_B=4 Pa·s, and G=30 Pa.

Presented in Fig. 5 are the numerical results of wave attenuation computed using the visco-elastic–plastic model

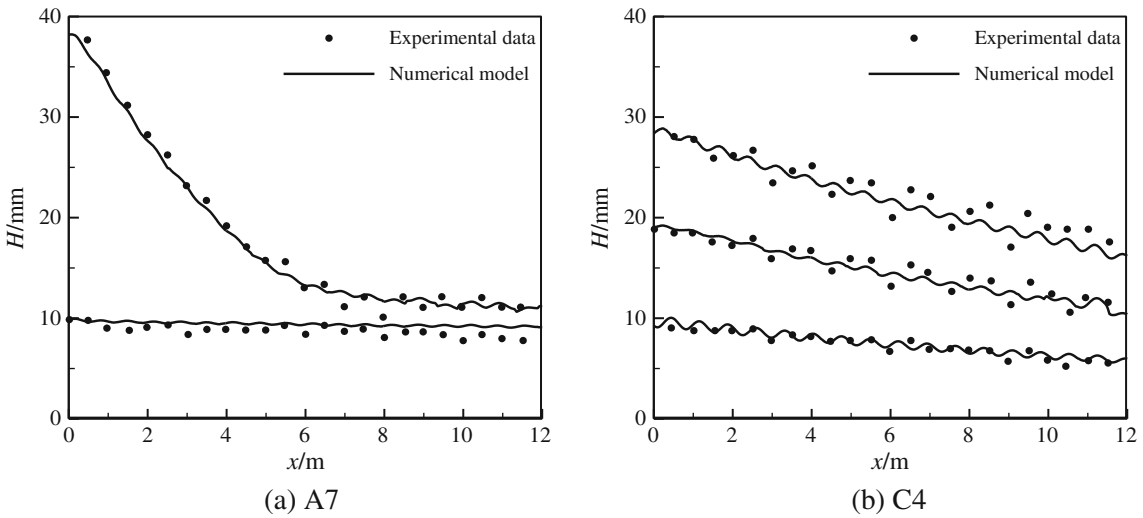

Fig. 5 Computed wave height along x axis by the visco-elastic–plastic model

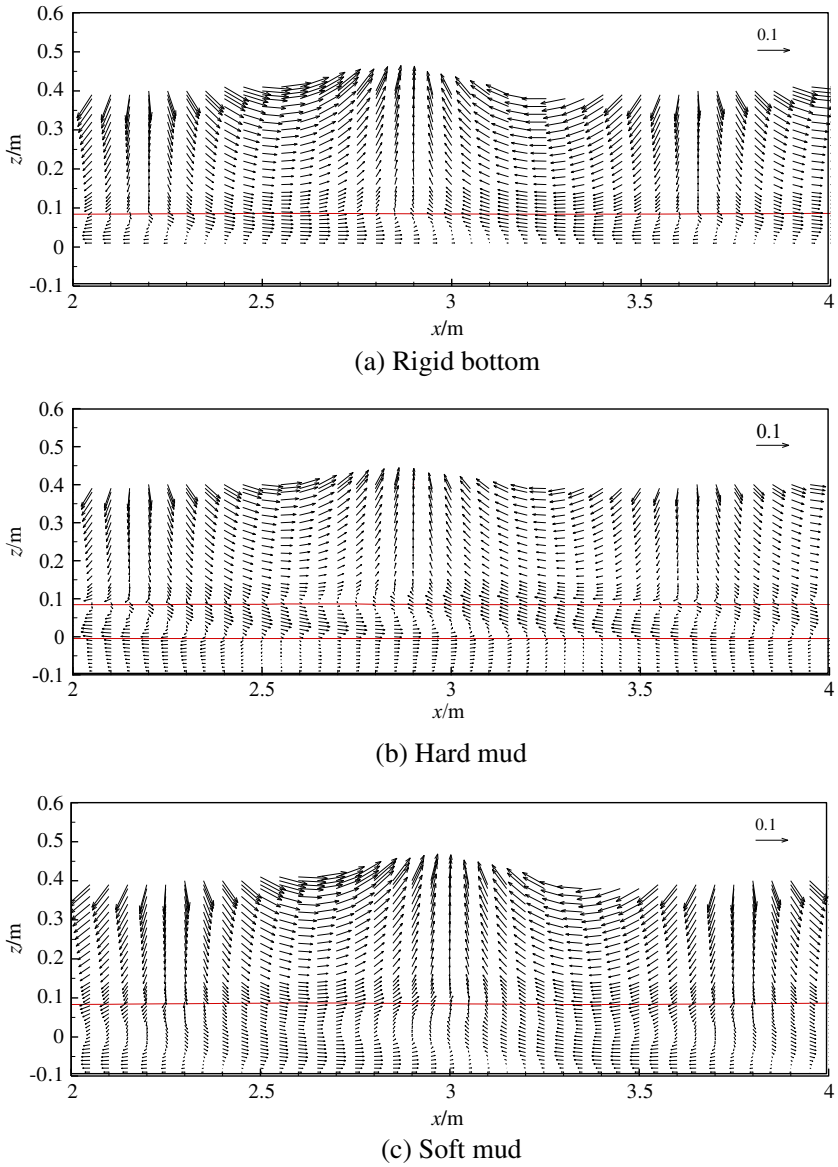

Fig. 6 Numerical result of the velocity distribution

for the mud, in comparison with the experimental measurements. The agreement is now very satisfactory. It is necessary to point out that the good agreement for CASE A7 cannot be achieved by using the viscous mud model, no matter how the viscosity is adjusted.

4 Results and discussion

To investigate the influence of the underlying muddy seabed to the wave decay rate, three hypothetical cases were adopted. The computational domain is shown in Fig. 2, which is similar to the cases of Sakakiyama and Bijker (1989). Except for one additional layer beneath the fluid-mud layer, other geometrical parameters of the computational domain remain the same as the experimental cases of Sakakiyama and Bijker (1989). Mud

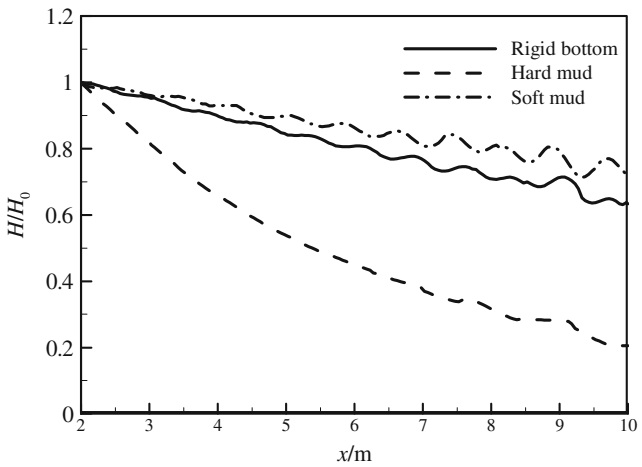

Fig. 7 Numerical result of the relative wave height

in both layers is described by the visco-elastic–plastic model. The mud density in the upper layer is 1,240 kg/m^3. Three different cases for the lower layer are considered: (1) rigid bottom, which represents that the underlying mud layer is of high degree of consolidation, i.e., of large density and hard to move; (2) a hard mud layer with relative larger density ρ_m= 1,370 kg/m^3 and thickness d_2=0.10 m; (3) a soft mud layer with density equal to that of the upper layer ρ_m=1,240 kg/m^3, and the thickness is d_2=0.10 m. Actually, there is only one mud layer in the rigid bed case and the soft bed case. The rheological parameters of the mud take the same values as in Table 3. The incident wave height is H=0.03 m, and the wave period is T=1.0 s.

Figure 6 shows the computed instantaneous velocity distribution within one wave length in the three different cases. The solid lines indicate the interfaces between water and mud layers. Comparing the instantaneous velocity distributions of the three cases, it can be seen that the gradient of velocity in the upper layer decreases as the lower layer becomes softer. Obviously, wave energy dissipation is caused by the viscosity and plasticity of the mud layers. It is found that the underlying layer plays a more important role in the two mud layer cases. Figure 7 shows the relative wave height distribution along the direction of wave propagation for the three different cases, in which the solid line shows the result in the case of rigid bottom, the dashed line shows the result in the case of an underlying layer of hard mud, and the dash dot line shows the result in the case of an underlying layer of soft mud. It is clear that the underlying layer significantly affects the wave height attenuation.

It is well known that the thickness of the mud layer is one of the important parameters for wave attenuation. It has been found that the wave damping rate first increases with the increase of mud layer thickness and then decreases when the mud layer thickness passes over a certain value. The maximum wave damping rate occurs when the mud thickness is around 1.25 times of the boundary layer thickness (Gade 1958; Dalrymple and Liu 1978; Ng 2000; Niu and Yu 2011). The boundary layer thickness is defined as $\delta_b = \sqrt{2\nu/\omega}$, in which ω is the angular frequency of wave, and ν is the kinematic viscosity of the fluid near the bed. Apparent kinematic viscosity is used for non-Newtonian fluid to estimate the boundary layer thickness. In this study, the boundary layer thickness is about 0.036 m corresponding to the soft mud and is 0.069 m corresponding to the hard mud. In the case of rigid bottom, the mud layer thickness is about 2.5 times of boundary layer thickness. In the case of soft mud, the mud layer thickness is obviously larger than that in the case of rigid bottom, so the wave damping rate is relatively small.

In the case of a movable hard mud layer beneath the fluid-mud layer, the viscosity and plasticity of the underlying hard mud layer are much larger than those of the upper mud layer, and most energy is dissipated in this layer. It can be seen that the ratio of the hard mud layer thickness to the boundary layer thickness in this case is about 1.3, which is near the value corresponding to the maximum wave damping rate. So the case with a hard underlying mud layer results in remarkable wave decay, compared to the case with a soft underlying mud layer, as shown in Fig. 7. The results are consistent with the results of the one mud layer cases shown in Fig. 5a and b.

5 Conclusions

A numerical model for wave propagation over a multilayered muddy seabed was developed, based on the governing equations of incompressible flows. The numerical scheme was directly extended from the SMAC method and is extendable to a variety of mud rheology models. The model was validated with the experiments carried out by Sakakiyama and Bijker (1989), and the numerical results were in good agreement with the experimental data. The comparison of the results from the viscous mud model and from the visco-elastic–plastic mud model shows that the visco-elastic–plastic model is more suitable than the viscous model, especially for the mud of relatively large density. Then, the numerical model is used to investigate the wave induced movement of a fluid-mud layer with different bottom conditions and its influence on wave decay. It is found that the underlying mud layer also plays an important role in the wave–mud interaction and greatly affects the wave decay rate. Therefore, in order to predict wave decay on muddy seabed with satisfactory accuracy, not only the thickness and the rheological parameters of the upper fluid-mud layer, but also the properties of the lower movable mud layer, should be determined accurately.

Acknowledgments The authors would like to acknowledge the support by the National Natural Science Foundation of China under the grant No. 51109119 and the Specialized Research Fund for the Doctoral Program of Higher Education of China under the grant No. 20110002120019.

References

An NN (1993) Mud mass transport under wave and current. PhD Thesis, Department of Civil Engineering, Yokohama National University, Yokohama, Japan

Dalrymple RA, Liu PL-F (1978) Waves over soft muds: a two-layer fluid model. J Phys Oceanogr 8:1121–1131

Gade HG (1958) Effects of a nonrigid, impermeable bottom on plane surface waves in shallow water. J Mar Res 16(2):61–82

Hall K, Oveisy A (2007). Wave evolution on fluid mud bottom. *Coastal Sediments'07—Proceedings of 6th International Symposium on Coastal Engineering and Science of Coastal Sediment Processes*, New Orleans, LA, United States.

Hirt CW, Nichols BD (1981) Volume of fluid (VOF) method for the dynamics of free boundaries. J Comput Phys 39:201–225

Huang L, Ng C-O, Chwang AT (2006) A Fourier–Chebyshev collocation method for the mass transport in a layer of power-law fluid mud. Comput Methods Appl Mech Eng 195:1136–1153

Jiang L, Zhao Z (1989) Viscous damping of solitary waves over fluid-mud seabeds. J Waterw Port Coast Ocean Eng 115(3):345–362

Jiang L, Kioka W, Ishida A (1990) Viscous damping of cnoidal waves over fluid-mud seabed. J Waterw Port Coast Ocean Eng 116(4):470–491

Maa JPY, Mehta AJ (1988) Soft mud properties: Voigt model. J Waterw Port Coast Ocean Eng 114(6):765–770

Macpherson H (1980) The attenuation of water waves over a non-rigid bed. J Fluid Mech 97(4):721–742

Mehta AJ, Lee S-C, Li Y (1994) Fluid mud and water waves: a brief review of interactive processes and simple modeling approaches. Florida

Mei CC, Liu K-F (1987) A Bingham-plastic model for a muddy seabed under long waves. J Geophys Res 92(C13):14581–14594

Ng C-O (2000) Water waves over a muddy bed: a two-layer Stokes' boundary layer model. Coast Eng 40:221–242

Niu X (2008) Dynamic interaction between surface water waves and muddy seabed. PhD Thesis, Tsinghua University, Beijing, China (in Chinese)

Niu X, Yu X (2008a) A practical model for the decay of random waves on muddy beaches. J Hydrodyn 20(3):288–292

Niu X, Yu X (2008b) Visco-elastic–plastic model for muddy seabeds. J Tsinghua Univ (Sci & Tech) 48(9):37–41 (in Chinese)

Niu X, Yu X (2010) A numerical model for wave propagation over muddy slope. *32nd International Conference on Coastal Engineering (ICCE 2010)*, Shanghai, China.

Niu X, Yu X (2011) Numerical study on the movement of muddy seabed under waves. *Proceedings of the Sixth International Conference on Asian and Pacific Coasts (APAC 2011)*, Hong Kong, China.

Rogers WE, Holland KT (2009) A study of dissipation of wind-waves by mud at Cassino Beach, Brazil: prediction and inversion. Cont Shelf Res 29:676–690

Sakakiyama T, Bijker EW (1989) Mass transport velocity in mud layer due to progressive waves. J Waterw Port Coast Ocean Eng 115(5): 614–633

Shibayama T, Okuno M, Sato S (1990) Mud transport rate in mud layer due to wave action. *Proceeding 22nd International Conference on Coatal Engineering*, 3037–3049

Winterwerp JC, Graaff RFd, Groeneweg J, Luijendijk AP (2007) Modelling of wave damping at Guyana mud coast. Coast Eng 54(3):249–261

Zhao ZD, Lian JJ (1994) On the change of wave parameters for water waves propagating over a muddy bottom. J Tianjin Univ 27(5):521–528 (in Chinese)